**PETROVIETNAM JOURNAL**
Volume 6/2020, pp. 22 - 29
ISSN 2615-9902

# CLASSIFICATION AND PETROPHYSICAL CHARACTERISATION OF MIOCENE CARBONATE RESERVOIR IN WELL RR02, SONG HONG BASIN, VIETNAM

**Ta Thi Hoa, Nguyen Hoang Anh**
Vietnam Petroleum Institute (VPI)
Email: anhnh@vpi.pvn.vn

## Summary

This study performs an integrated method using thin section and well log data to determine rock fabrics and their relationship with the rock pore system in Miocene carbonate reservoirs of well RR02, southern Song Hong basin, Vietnam. By thin section analysis, mineral components and pore types of carbonate rocks were determined, creating a basis for carbonate classification and grouping samples into different petrophysical classes. Zoning, identification of dominant changing trend of the petrographic composition and porosity estimation were then conducted based on the combination of different standard log curves, including gamma ray (GR), photoelectric factor (PEF), neutron porosity (NPHI), density (RHOB) and sonic (DT). Four types of rock fabrics were diagnosed along a nearly 90m-thick carbonate reservoir, namely, grainstone, grain-dominated packstone, wackstone and boundstone. Two main pore types were found corresponding to each identified carbonate fabric, including interparticle and vuggy pores estimated by well log interpretation in the range of 5.9% to 10% and 2.9% to 21.5%, respectively. In well RR02, carbonate reservoir was mostly formed by limestone and could be divided into 2 zones with the lower affected by dolomitisation proved by the results of petrographic analysis, log curve characteristics and well log interpretation.

**Key words:** Carbonate reservoir, petrographic analysis, well log interpretation, porosity, dolomite.

## 1. Introduction

The study area is located about 80 km offshore Vietnam in the southern part of the Song Hong basin (Figure 1). The Miocene carbonate is an isolated platform, established on the horst structural high throughout the Early and Middle Miocene and ending in the Late Miocene due to the development of siliciclastic sediment, affected by regional uplift from the West. The estimated gas reserve is about 4 TCF with approximately 30% $CO_2$.

Petrophysical properties of carbonate reservoirs are more difficult to be determined than those of siliciclastic reservoirs because of their heterogeneity. The carbonate pore network that controls the petrophysical properties, such as porosity, permeability and saturation, is distributed irregularly from well to basin scale and classified into various classes, including interparticle and vuggy porosity [2]. In order to classify carbonate rock types and characterise their petrophysical properties, core samples are necessary to be collected and petrographic analysis using thin sections also needs to be carried out. 17 thin section samples obtained from Miocene carbonate reservoir of well RR02 were analysed using petrophysical microscope at the Laboratory Centre of the Vietnam Petroleum Institute (VPI-Labs). The thin section analysis provides information on main minerals, percentages of porosity, and rock fabric texture. Classification of carbonate rocks and their pore types were classified and compared using Folk's, Dunham's, Choquette & Pray's and Lucia's classification charts [3 - 7]. Based on Lucia's scheme [7], petrophysical class was categorised for each sample corresponding to its fabric. In addition, standard log curves were used for zoning and well log interpretation, including GR (gamma ray), RD (resistivity), NPHI (neutron), RHOB (bulk density), DTC (sonic), and PEF (photoelectric factor). Different cross-

*Date of receipt: 26/3/2020. Date of review and editing: 27/3 - 6/5/2020.*
*Date of approval: 5/6/2020.*

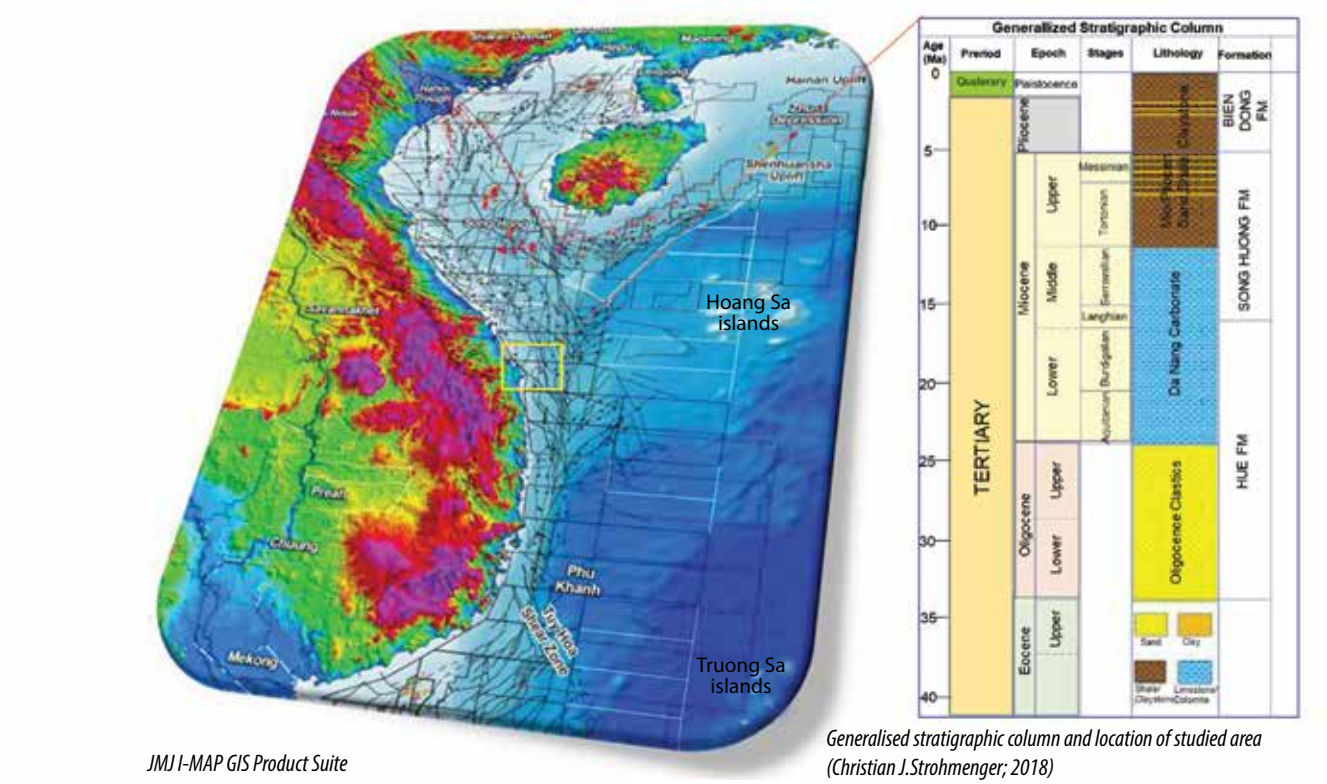


JMJ I-MAP GIS Product Suite

Generalised stratigraphic column and location of studied area (Christian J.Strohmenger; 2018)

***Figure 1.*** *Location map and general stratigraphic column of the study area [1].*

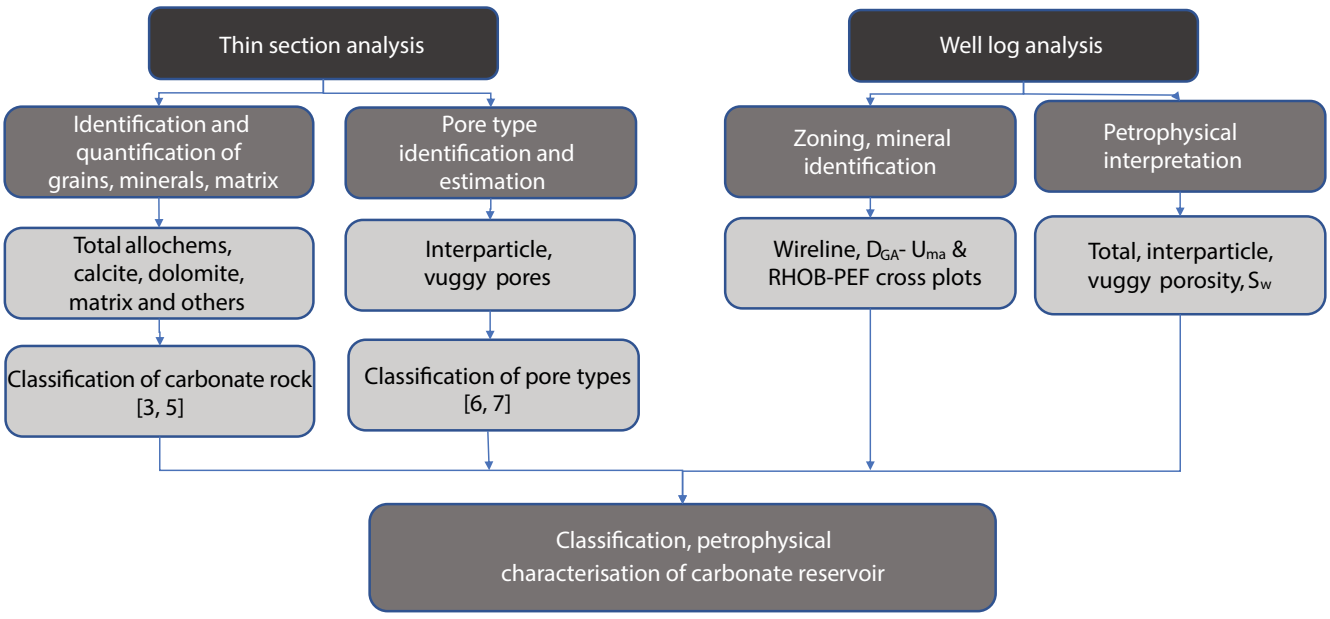


***Figure 2.*** *Methodology for the study.*

plots were also applied to determine the changing trend of main mineral components versus depth, including apparent matrix volumetric photoelectric factor ($U_{ma}$) - apparent matrix grain density ($D_{GA}$) introduced by Burke et al. [8, 9] and PEF vs RHOB proposed by Schlumberger [10]. $U_{ma}$ and $D_{GA}$ are shown in Equation (1):

$$U = PEF \times \frac{RHOB + 0.1883}{1.0704}$$

$$U_{ma} = \frac{U - U_f \times \Phi_t}{1 - \Phi_t} \quad (1)$$

$$D_{GA} = \frac{RHOB - RHOB_f \times \Phi_t}{1 - \Phi_t}$$

Where:

PEF: Photoelectric factor (b/e);

$\phi_t$: Total porosity (fraction);

$RHOB_f$: Pore fluid density; 0.692 g/cc for gas interval and 1.0 g/cc for water interval;

$U_f$: Pore fluid volumetric factor 0.398 (barns/cc);

$U_{ma}$: Apparent matrix volumetric cross section (barns/cc).

The well log interpretation was conducted to provide detailed petrophysical information such as porosity, water saturation and net pay along the wellbore (Figure 2). Density, neutron and alternative sonic methods were used to estimate porosity while the gas effect was taken into account by inputting gas density in related porosity models. In carbonate rocks, the type representing interparticle porosity [4] and vuggy porosity ($\phi_v$) is calculated by subtracting interparticle porosity (sonic porosity) from total porosity (neutron - density porosity).

## 2. Results and discussion

Results from thin section analysis and well log interpretation have been utilised to classify the rock fabrics and characterise the petrophysical properties of this reservoir. Figure 3 shows that collected samples considerably comprise carbonate allochems, sparry cement and micrite. By thin section analysis, total porosity was estimated from good to excellent as ranging from 10% to 25.9% in total, in which pores were mostly formed by separate vugs, interparticles, intercrystals and touching vugs. Vuggy porosity was approximately from 4% to 15.3%, formed by intraparticle, moldic pores and dissolution of lime mud matrix and cement. Besides, interparticle porosity, which is formed by the arrangement of allochems and dissolution of previous micrite and sparry cement filled among grains, varied from 0 to 17.3%. Fracture pores were also locally noted with minor value (Figure 4).

According to Folk [3], 7 rock samples were recognised as bio-micrite and 9 samples were interpreted as unsorted bio-sparite, in which 4 samples were dolomitised partly with medium crystal size. There is only one thin section determined as bio-lithite and it was also affected by dolomitisation. Considering the textures named by Dunham [5], 14 samples were interpreted as packstone against one sample of grainstone and one of wackstone. There is only one specimen recorded as boundstone with characteristic of encrusted texture, in which red algae and echinoderm were bound together during deposition. The dolomitisation was also encountered in 5 samples at depths of 1794.25 m, 1798.75 m, 1804.75 m, 1814.51 m and 1814.77 m with dolomite crystal size varying from 10.5 µm to 60 µm. Pore networks of this well were classified based on Choquette & Pray's scheme [6]. There is a predominance of intraparticle

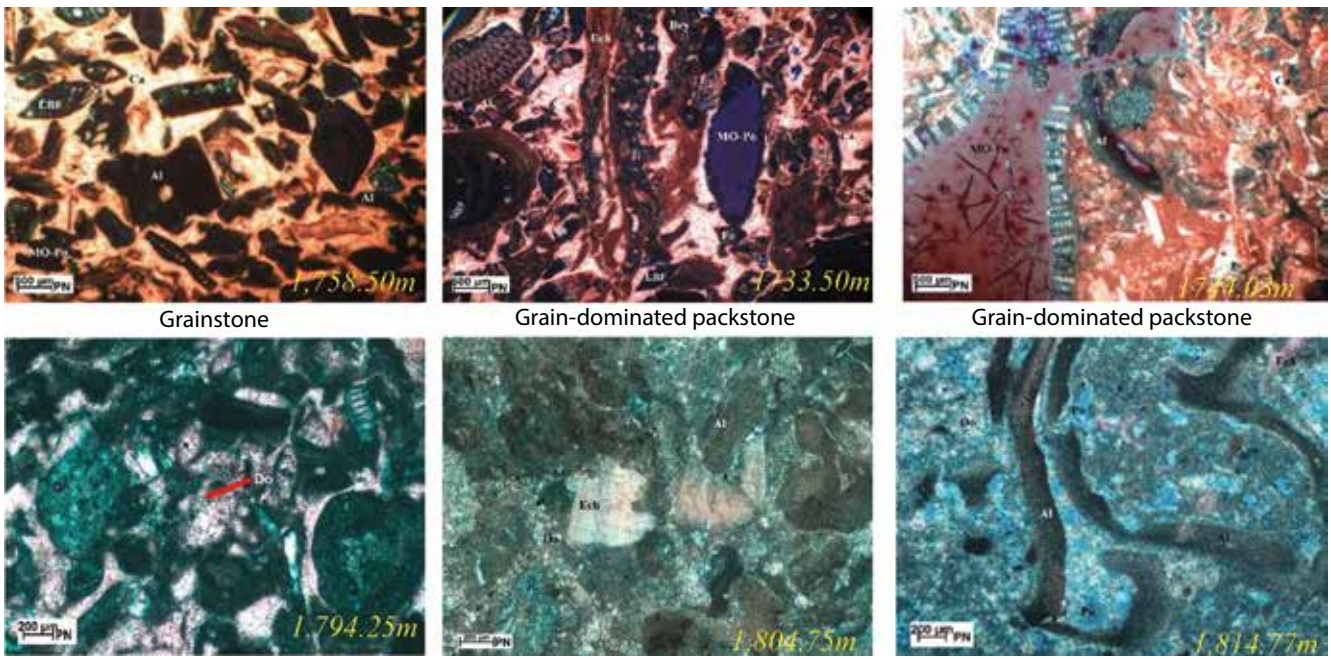


Grainstone | Grain-dominated packstone | Grain-dominated packstone

Grain-dominated packstone dolomitic | Boundstone dolomitic | Wackstone dolomitic

***Figure 3.*** *Thin section analysis of RR02 samples.*

over interparticle and mold pore types. For the rocks suffered from dolomitisation, intercrystal porosity was also recorded. Besides, the processes such as solution, cementation, and direction or stage (enlarged, reduced or filled) of porosity evolution, were combined with the pore size namely mesopore for rock description. These terms were applied to classify the pore network of 17 rock samples. Based on the classification of Lucia [7], carbonate rocks could be divided into 2 groups: Group I (grain-dominated fabric) includes 15 samples, in which 14 samples are grain-dominated packstone and one sample indicates grainstone fabric. Group II (mud-dominated fabric) consists of 2 samples with fabric of wackstone and boundstone for each. Rocks affected by dolomitisation were considered with dolomite crystal size along with grain size. Rocks were then put into different classes according to grain size, volumes of sparry calcite and mud. There are 3 classes with 14 samples belonging to Class 2, 1 sample to Class 1 and 2 others to Class 3. Table 1 and Figure 5 display the comparison of different carbonate classification schemes applied for carbonate rocks of well RR02.

Three zones were divided corresponding to the well log data of well RR02, in which the seal layer overlies on Miocene carbonate layers. Zone 1 was defined with the main lithology of shale based on the high value of GR (101 - 136 API), low value of RD from 1.7 Ohm.m to 3.8 Ohm.m, PEF from 3.5 b/e to 5.6 b/e, DTC from 98 µs/ft to 130 µs/ft, and N-D gap around 30 - 34%. The lithology of Zone 2 was diagnosed as limestone since GR is quite low from 23 API - 50 API, PEF from 5.0 b/e to 6.2 b/e, DTC from 57 µs/ft to 85 µs/ft, N-D from 0% to 10%. Zone 3 was interpreted as dolomitised limestone because of PEF values from 4.2 b/e to 5.5 b/e, and N-D ranging from 3% to 15%. The basic rule to classify limestone and dolomitised limestone is the overlay and separation of NPHI and RHOB log curves. In Zone 2, these 2 logs overlie each other in contrast to their separation in Zone 3 (Figure 6).

Cross-plots of RHOB versus PEF and $U_{ma}$ versus $D_{GA}$ were applied to clarify lithology change for Zone 2 and Zone 3. PEF vs RHOB cross-plot shows the predominance of limestone with high value of porosity, varying from 5% to 25%. It is clear that using the raw curves as RHOB and PEF indicates all the samples points belong to the limestone lithology without neither dolomite nor other lithology. In contrast, the $U_{ma}$ vs $D_{GA}$ cross-plot demonstrates the general changing trend of main minerals for Zone 2 as calcite with the concentration of most data at calcite vertex while Zone 3 presents a part of calcite that has been slightly affected by dolomitisation. The porosity values derived by well log interpretation (total porosity: 31.58%; interparticle: 10.04%; vug: 21.53%) including both interparticle and vuggy porosity are much higher than those of Zone 2 (total porosity: 18.79%; interparticle: 5.88%; vug: 12.92%). The using of $U_{ma}$ vs $D_{GA}$ cross-plot illustrates to be more effective approach

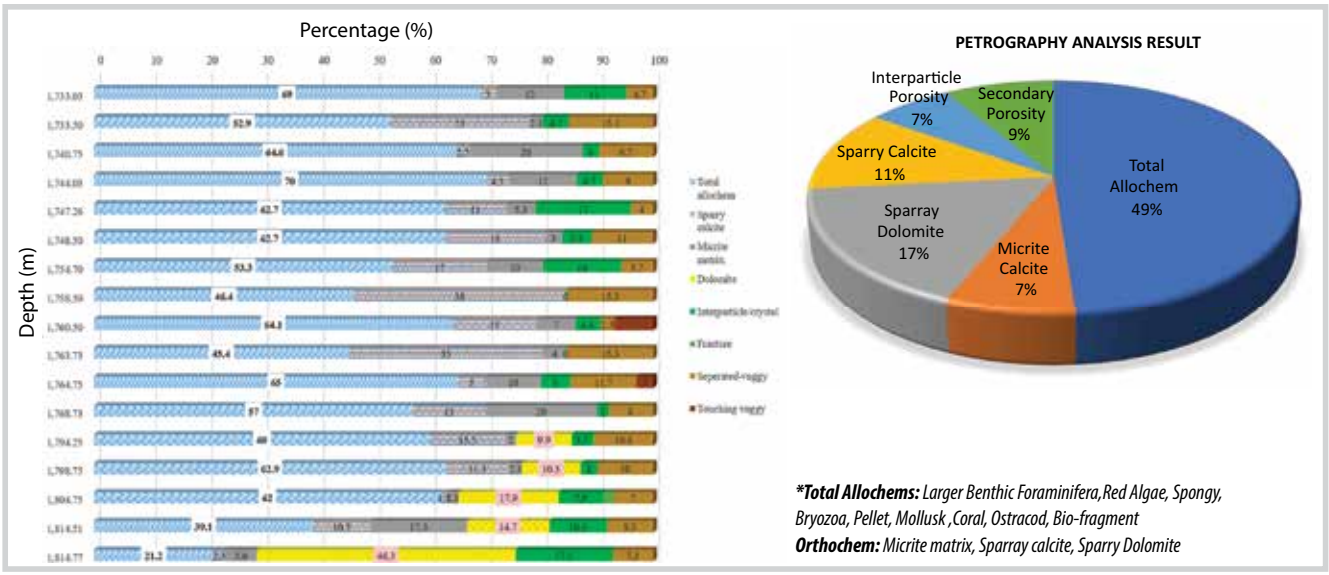


***Figure 4.*** *Result of thin section analysis, well RR02: Allochems with different shapes and sizes constitute a considerable proportion, ranging from 21.2% to 70% of total rock volume. The components of allochems include larger benthic foraminifera, red algae, spongy, bryozoa, pellet, mollusk, echinoderm, coral, ostracod and unidentified bio-fragment. Sparry calcite was present in large amount with significantly non-ferroan calcite from 3% to 38%, non-ferroan dolomite from 9.9% to 46.3%. Sparry cement was commonly found with morphologies of isopachous to mosaic whereas dolomite was present as rhombic, euhedral to anhedral, fine to medium crystal size. Micrite matrix ranges from 2% to 20% and partly experienced a dolomitisation, converting lime mud matrix from subhedral to euhedral rhombic dolomite.*

***Table 1.*** *Comparison of carbonate classification using different schemes*

| Sample No. | Depth | Classification of Carbonate Rocks | | Classification of Pore types | | | | | | | |
|---|---|---|---|---|---|---|---|---|---|---|---|
| | | | | | Lucia [7] | | | | | | |
| | | | | | | | | Porosity | | | |
| | | Folk [3] | Duham [5] | Choquette & Pray [6] | Fabric | Grain size/Crystal size (μm) | Petrophysical Class | Interparticle | Fracture | Separated-Vug | Touching Vug |
| 1 | 1733.03 | Packed Biomicrite (7) | Packstone (14) | Intraparticle/Interparticle pores | Fossil GDP(14) | 400 - 500 | Class 2 | 11 | 0.3 | 4.7 | |
| 2 | 1733.5 | Unsorted Biosparite | | **Moldic, Intraparticle/Interparticle** pores | | 300 - 500 | | 4.7 | | 15 | |
| 3 | 1740.75 | Packed Biomicrite | | **Solution enlarged-Interparticle**/Intraparticle pores | | 240 - 500 | | 3 | | 9.7 | |
| 4 | 1744.03 | | | Moldic, Interparticle/Intraparticle pores | | 400 - 500 | | 4.7 | | 9 | |
| 5 | 1747.26 | Unsorted Biosparite(9) | | Intrarparticle/Interparticle pores | | 400 - 501 | | 17 | | 4 | |
| 6 | 1748.5 | | | Moldic, Intraparticle pores | | 400 - 502 | | 5.3 | | 11 | |
| 7 | 1754.7 | | **Grainstone (1)** | Moldic, Intraparticle pores | **Grainstone (1)** | 340 - 500 | | 14 | | 5.7 | |
| 8 | 1758.5 | | Packstone | Intraparticle pores | Fossil GDP | 300 - 500 | **Class 1** | Tr | 0.3 | 15.3 | |
| 9 | 1760.5 | | | Solution enlarged- Interparticle, Interparticle, Intraparticle pores | | 350 - 500 | Class 2 | 4.3 | 0.3 | 2.3 | 7 |
| 10 | 1763.73 | | | Interparticle/Intraparticle pores | | 440 - 500 | | Tr | 0.3 | 15.3 | |
| 11 | 1764.75 | Packed Biomicrite | | Solution enlarged-Intraparticle/Interparticle pores | | 340 - 500 | | 5 | 0.3 | 11.7 | 3 |
| 12 | 1768.73 | | | Moldic, Interparticle/Intraparticle pores | | 200 - 500 | | 2 | | 8 | |
| 13 | 1794.25 | Dolomitised Biosparite | Dolomitised Packstone | **Moldic, solution-enlarged intraparticle, intraparticle** pores | GDP Dolomitic | 200 - 500 | | 3.7 | 0.3 | 10.6 | |
| 14 | 1798.75 | | | Intraparticle pores | | 200 - 500 | | 3 | | 10 | |
| 15 | 1804.75 | **Dolomitised Biolithite (1)** | **Dolomitised Boundstone(1) (red algae and echinoderm)** | Intercrystal, cement-reduced growth-framework | **Boundstone Dolomitic (1)** | >200 | **Class 3** | 7.9 | 2 | 7 | |
| 16 | 1814.51 | Dolomitised Biomicrite | Dolomitised Packstone | Intercrystal, intrapaticle pores | GDP Dolomitic | 300 - 500 | Class 2 | 10.3 | | 8.3 | |
| 17 | 1814.77 | | **Dolomitised Wackstone(1)** | Intercrystal pores | **Wackstone(1)** | 100 - 300 | **Class 3** | 17.3 | | 7.3 | |

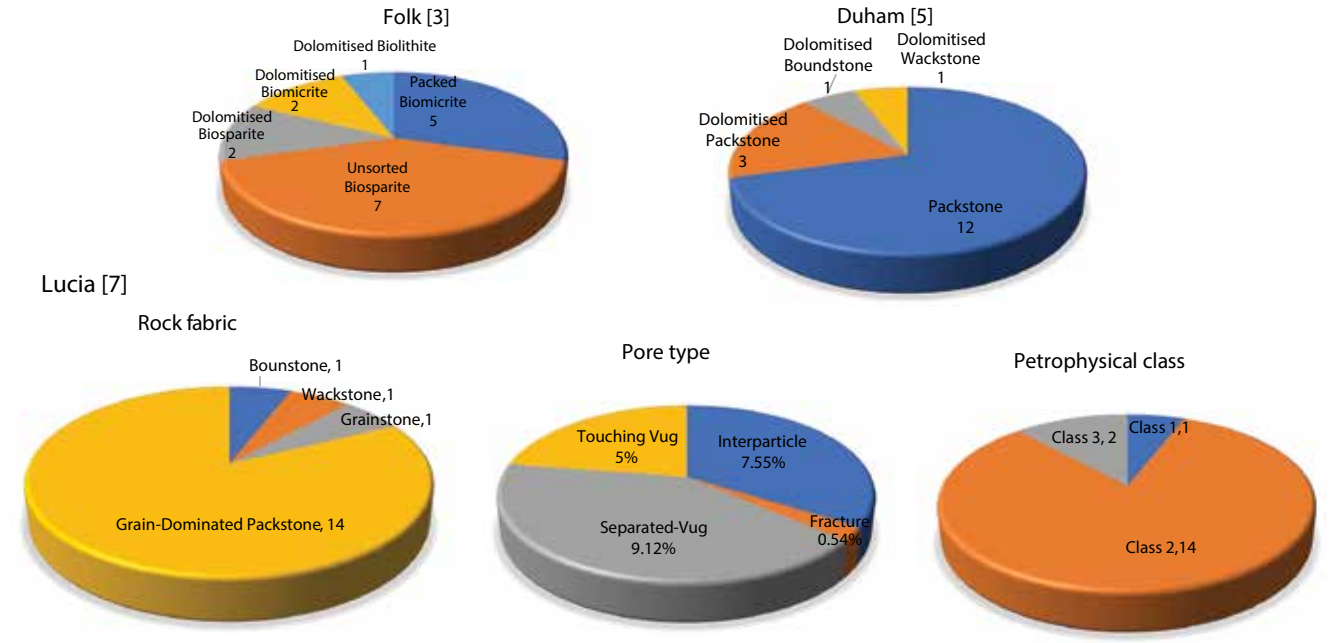


***Figure 5.*** *Summary of carbonate classification by different methods.*

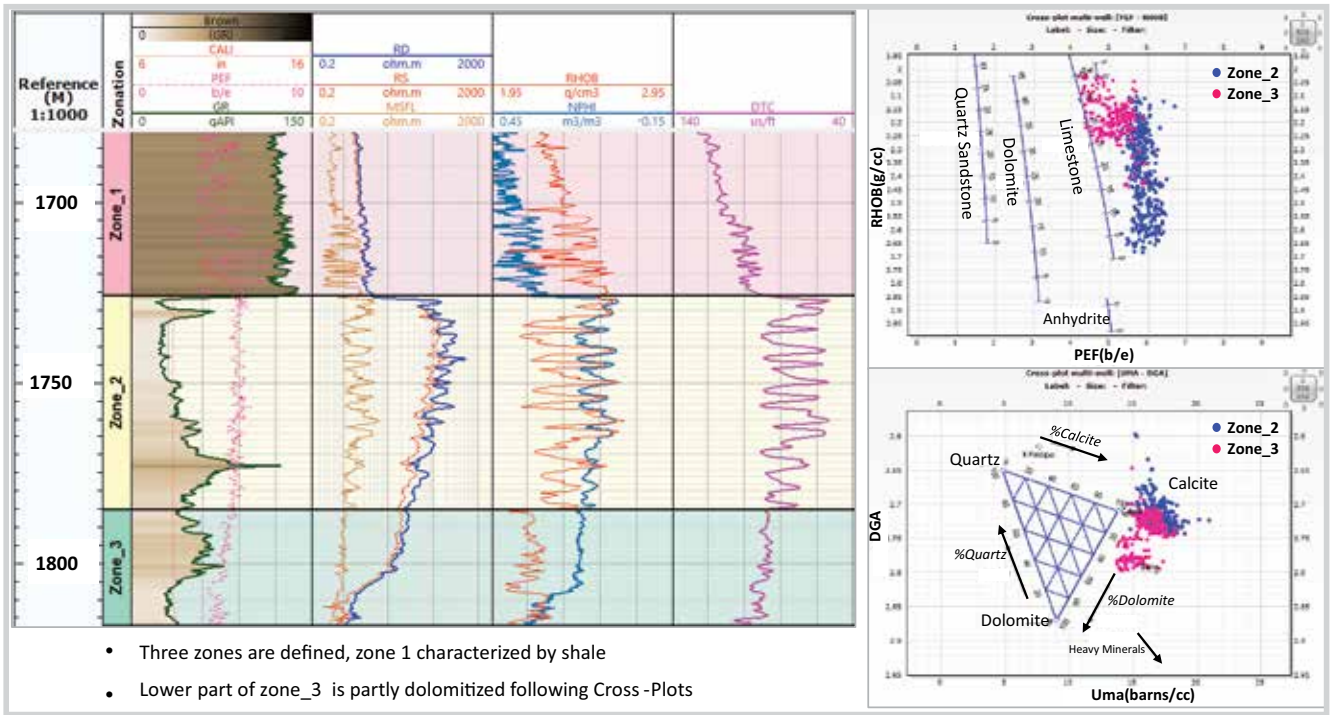


***Figure 6.*** *Zoning and identifying the changing trend of lithology composition based on well log.*

to classify the general changing trend of limestone and dolomite than the PEF-RHOB cross-plot, which has been verified by results of both petrography analysis and well log interpretation.

The well log interpretation results in Zone 2 with 38.9 m net pay, 21.4% effective porosity and 15.3% water saturation and in Zone 3 with 28.3 m net pay, 29.1% effective porosity and 27.8% water saturation. Gas water contact (GWC) is interpreted as 1807 mMD as Figure 7.

The maximum flooding surface (MFS) is interpreted at 1,772 mMD as the highest gamma curve marking the transition of relative sea level from transgression to regression (Figure 7). This could be linked with the reactivation of strike-slip activities of Song Hong fault in the Late Miocene. The lower part of MFS is interpreted as deep marine environment in transgressive system tract (TST) with a high rate of carbonate production characterised by abundant red algae and larger benthic

foraminifera. This part includes thick carbonate with higher poroperm properties compared to thinner carbonate layers interbedded with carbonate cement layers (2 - 3 m) above MFS. The upper part of MFS deposits in a high stand system tract (HST) which is bounded by MFS and sequence boundary (SB) as top of Zone 2 in shallow water depth with upward stacking patterns. The extensive porosity destructive characterised by interbedded low-poroperm layers resulted from significant marine cementation in HST period. The lower effective porosity in Zone 2 compared with that of Zone 3 from core analysis and well log interpretation supports the above interpretation. Top of Zone 2 is marked by about 3 m of tight carbonate layer formed when the carbonate was exposed as karst surfaces and reservoir has been filled by carbonate cement through by meteoric water realm. The thick shale zone above carbonate formation illustrates the transition from shallow to deep marine environment. Results of the petrography analysis and well log response represent small fracture occurrence with main interparticle porosity and secondary porosity as vugs which suggests less tectonic activities affected on this carbonate formation.

Figure 6 shows all integrating results from all pertinent data of well RR02. As the petrographic analysis, the dissolution of allochems and precipitation of calcite cements are the main diagenesis processes recorded from RR02 samples. The effective porosity is well matching with the core porosity in track 7 with higher porosity in Zone 3. The increasing trend of dolomite content occurred below the depth of 1,770 mMD (light blue fill in track 4), which is consistent with the higher secondary porosity resulting from well log interpretation (yellow fill in track 8). Secondary porosity derived from well log interpretation is always higher than those estimated from thin section analysis. The reason could be the well log method reflects the response of the whole pore space in their investigation depth, whereas the thin section just provides information of two dimensions rock slab within a small area.

As above-mentioned, the dolomite distribution mostly observed in Zone 3 by integrating both thin section analysis and $U_{ma}$ vs $D_{GA}$ cross-plot. The question needs to be answered is why dolomite occurrence only has an increasing tendency towards the lower interval and whether it is correlated with petrophysical properties in RR02. It could be explained that high $CO_2$ content, confirmed by the testing result, is diffused from the hydrocarbon reservoirs down into water bearing zone resulting in the secondary leaching in Zone 3. The diffusion process therefore causes dissolution of the fossil assemblage, mainly made by red algae and larger benthic foraminifers, to enrich the environment with Mg-calcite which partly provoked the dolomitisation proved by petrography analysis and well log interpretation results. This result also explains why the dolomite component was less observed in the above interval than in Zone 2, where less red algae and LBF were found, and which is located quite far from the water contact with multiple

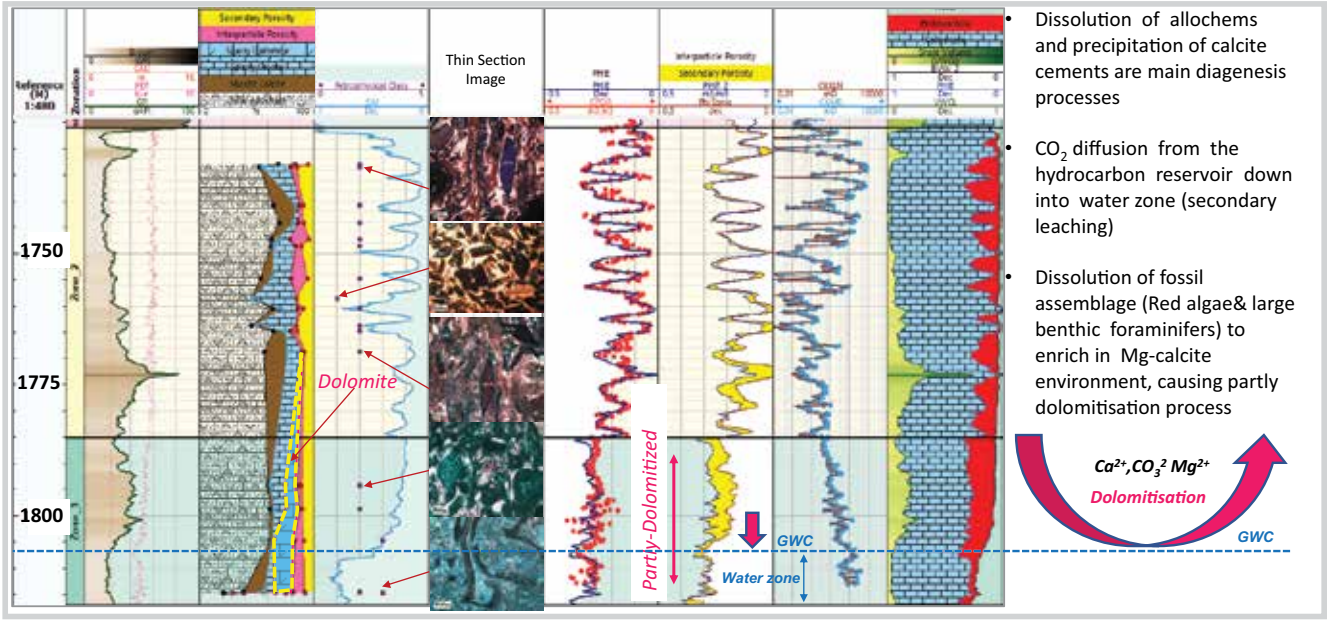


***Figure 7.*** *Well log interpretation result in RR02.*

barrier carbonate cement layers. Most of dolomite crystals in the lower part of Zone 3 observed from thin section analysis are euhedral (planar-e) in eogenesis process and play a significant role to enhance reservoir properties in well RR02. Details of zone division, log response values and dolomitisation process are displayed and summarised in Figure 7.

**3. Conclusions**

Miocene carbonate reservoirs, less experienced tectonic activities, were formed by grain-dominated fabric, including grain-dominated packstone and grainstone with mainly allochem, sparry calcite, sparry dolomite and micrite matrix. Petrography analysis and useful $U_{ma}$ - $D_{GA}$ cross-plot are utilised to efficiently determine the general changing trend of the lithology composition in carbonate successions. Porosity estimated by well log interpretation in well RR02 is from high to excellent, 2 - 38% (avg 20%), with diverse pore types. Secondary porosity by cementation, micritisation, acidification, dissolution and acidification processes is up to 19% (avg 8%). Secondary leaching of the Mg-rich red algae and LBFs caused by $CO_2$ diffusion from the hydrocarbon reservoir down into the water bearing zone could be the key factor for the dolomitisation process occurring in the lower part. The integrated method used in this research proves a significant result on carbonate reservoir characterisation and it can be applied for other wells in this carbonate field for a better support to the above statement. Full assessment of petrophysical properties of rock in consideration of other parameters including permeability and related reservoir behaviour parameters needs to be carried out to have an insight about this heterogeneity reservoir.

**References**

[1] Christian J.Strohmenger, Lori Meyer, David S.Walley, Mazlina Md Yusoff, Donald Y.Lyons, Jacqueline Sutton, John M.Rivers, Beata von Schnurbein, and Nguyen Xuan Phong, "Reservoir characterisation of the Middle Miocene Ca Voi Xanh isolated carbonate platform", *Petrovietnam Journal*, Vol. 6, pp. 10 - 24, 2018.

[2] Vivian K.Bust, Joshua U.Oletu, and Paul F.Worthington, "The challenges for carbonate petrophysics in petroleum resource estimation", *SPE Reservoir Evaluation & Engineering*, Vol. 14, No. 1, pp. 25 - 34, 2011. DOI: 10.2118/142819-PA.

[3] Robert L.Folk, "Spectral subdivision of limestone types", *Classification of carbonate rocks - A symposium*, AAPG Memoir, Vol. 1, pp. 62 - 84, 1962. DOI: 10.1306/M1357.

[4] F.J.Lucia, "Petrophysical parameters estimated from visual descriptions of carbonate rocks: A field classification of carbonate pore space", *Journal of Petroleum Technology*, Vol. 35, No. 3, pp. 629 - 637, 1983. DOI: 10.2118/10073-PA.

[5] Robert J.Dunham, "Classification of carbonate rocks according to depositional texture", *Classification of carbonate rocks - A symposium*, AAPG Memoir, Vol. 1, pp. 108 - 121, 1962. DOI: 10.1306/M1357.

[6] Philip W.Choquette and Lloyd Charles Pray, "Geologic nomenclature and classification of porosity in sedimentary carbonate", *AAPG Bulletin*, Vol. 54, No. 2, pp. 207 - 250, 1970.

[7] F.Jerry Lucia, "Rock-fabric/petrophysical classification of carbonate pore space for reservoir characterization", *AAPG Bulletin*, Vol. 79, No. 9, pp. 1275 - 1300, 1995. DOI: 10.1306/7834D4A4-1721-11D7-8645000102C1865D.

[8] J.A.Burke, R.L.Campbell, and A.W.Schmidt, "The litho-porosity cross plot - A method of determining rock characteristics for computation of log data", *SPE Illinois Basin Regional Meeting, Evansville, Indiana, 30 - 31 October, 1969*.

[9] Robert Cluff, Suzanne Cluff, Ryan Sharma, and Chris Sutton, "A deterministic lithology model for the green river-upper wasatch interval of the Uinta basin", *AAPG Annual Convention & Exhibition 2015, Denver, Colorado, 31 May - 3 June, 2015*.

[10] Schlumberger, *Log interpretation*. Principles/ Applications. Texas: 1989.